Light absorption spectrum of two-dimensional Mott insulators

Hisashi Itoh, Akira Takahashi, and Masaki Aihara
Graduate School of Materials Science, Nara Institute of Science and Technology, 8916-5, Takayama-cho, Ikoma, Nara 630-0101, Japan
(Received 7 October 2005; revised manuscript received 28 November 2005; published 16 February 2006)

We theoretically investigate the light absorption spectrum of two-dimensional (2D) Mott insulators. We employ the numerical diagonalization method to calculate the light absorption spectrum with using the effective Hamiltonian for the extended Hubbard model, which is valid when the on-site Coulomb interaction energy U is much larger than the nearest-neighbor transfer integral t and the nearest-neighbor Coulomb interaction energy V. For $V=0$, the absorption spectrum consists of a broad band with a width of about $16t$ and a sharp central peak, and the energy eigenstates contributing to the absorption spectrum do not have the antiferromagnetic (AF) spin order, when U is sufficiently larger than t. These features result from the spin-charge interplay inherent in the very strong correlation region where charge transfer term is dominant. With decreasing U/t, the peak structure in absorption spectrum becomes unclear and some low energy eigenstates have the AF spin order, as a result of the spin-spin interaction term. For large V/t, the dominant peak arises in the lower energy region of the spectrum. A large number of holon-doublon bound states, which have nearly the same charge but different spin structures, are responsible for this peak, in contrast to the conventional exciton state. This is also in contrast to the charge bound states in one-dimensional (1D) Mott insulators, where a single energy eigenstate dominates the optical transition moment as a result of the spin-charge separation. The essentially different absorption spectra between the 1D and 2D Mott insulators originate from the difference in the coupling between spin and charge degrees of freedom.

DOI: 10.1103/PhysRevB.73.075110 PACS number(s): 71.10.Fd, 71.35.Cc, 78.20.Bh

I. INTRODUCTION

Strongly correlated low-dimensional electron systems (SCLDES) exhibit various novel properties originating from strong Coulomb interaction between electrons. At half-filling, SCLDES are driven into Mott insulators by the strong correlation effect.[1,2] Since the optical gap originates from the strong correlation effect in the Mott insulators, the optically excited states are essentially different from those for conventional band insulators. Therefore, the optical properties of low-dimensional Mott insulators are expected to provide us with important information on the exotic nature of SCLDES.

Since both the positive and negative charges are generated simultaneously in the photoexcited states, it is important to take into account the charge binding effect arising from the attractive Coulomb interaction between both charges. Actually, the optical properties of conventional band insulators have been explained successfully within the Wannier-Mott exciton theory.[3] Recently, the importance of the charge binding effect is claimed also in low-dimensional Mott insulators.[4–7] However, since the physical properties of photogenerated charges in the Mott insulators are essentially different from those in the conventional band insulators as a result of the strong correlation effect,[2] the simple exciton theory is not applicable to the Mott insulators. In particular, it is important to recall that the charge motion in SCLDES is correlated with the spin degrees of freedom of the whole system, while an exciton in conventional band insulators is basically understood as a two-body problem between an electron and a hole. The interplay between the photogenerated charges and the spins will be a key to understand the optical properties of Mott insulators.

The light absorption spectrum in the one-dimensional (1D) Mott insulators has been investigated theoretically by several authors with using the Hubbard and the extended Hubbard models.[8–18] It has been shown that a pair of positive and negative spinless charges (a holon and a doublon) is photogenerated as a result of spin-charge separation, and an excitonlike bound state of the holon-doublon pair dominates the transition moment from the ground state when the Coulomb interaction between the nearest-neighbor sites is strong enough.[10–23]

In the two-dimensional (2D) strongly correlated electron systems, the spin and charge degrees of freedom are not fully separated, and it is considered that the interplay between these two degrees of freedom is the origin of various novel properties. Therefore, it is expected that the interplay will manifest itself in the light absorption spectrum in the 2D Mott insulators. The light absorption spectrum of the 2D Mott insulators has been investigated by several authors.[24–31] However, the main targets of these investigations are Drude and low energy structures of the optical conductivity in the doped case, and not the optically excited states in the Mott insulators. Furthermore, it has not been understood well how the spin-charge interplay and the charge binding affect on the light absorption spectrum.

We therefore focus our attention on the light absorption spectrum mainly in the 2D Mott insulators. The purpose of this paper is to clarify the unconventional properties of low-dimensional Mott insulators from the viewpoint of optical response. We adopt the effective Hamiltonian for the extended Hubbard model in the strong correlation case to analyze the charge binding effect on the spectrum, and calculate the light absorption spectrum with using the numerical diagonalization method. In order to further elucidate the characteristic feature inherent in the 2D Mott insulators, we also calculate the charge and spin correlation functions for some

energy eigenstates which are responsible for the major structures of light absorption spectrum. We also investigate the light absorption spectrum in the 1D Mott insulators, and compare the results with those in the 2D ones.

II. METHOD OF CALCULATIONS

To describe low-dimensional Mott insulators coupled with the light field, we consider the Hamiltonian given by

$$H = H_e + H_{e\text{-}p}. \tag{1}$$

As the electron Hamiltonian H_e, we adopt the extended Hubbard model given by

$$H_e = \hat{T} + \hat{U} + \hat{V}, \tag{2}$$

$$\hat{T} = -t \sum_{n,m,\sigma}^{\mathrm{NN}} c_{n,\sigma}^{\dagger} c_{m,\sigma}, \tag{3}$$

$$\hat{U} = U \sum_{n} c_{n,\uparrow}^{\dagger} c_{n,\uparrow} c_{n,\downarrow}^{\dagger} c_{n,\downarrow}, \tag{4}$$

$$\hat{V} = \frac{V}{2} \sum_{n,m}^{\mathrm{NN}} n_n n_m, \tag{5}$$

where $c_{n,\sigma}$ is the annihilation operator for an electron of spin σ at site n, t is the magnitude of the transfer integral between nearest-neighbor sites, U is the on-site Coulomb interaction energy, V is the Coulomb interaction energy between nearest-neighbor sites, $n_n = \Sigma_\sigma c_{n,\sigma}^{\dagger} c_{n,\sigma}$, and Σ^{NN} indicates the summation over nearest-neighbor sites. The electron-photon interaction part $H_{e\text{-}p}$ is given by

$$H_{e\text{-}p} = -\mathbf{A} \cdot \hat{\mathbf{J}}, \tag{6}$$

$$\hat{\mathbf{J}} = it \sum_{n,m,\sigma}^{\mathrm{NN}} (\mathbf{Q}_n - \mathbf{Q}_m) c_{m,\sigma}^{\dagger} c_{n,\sigma}, \tag{7}$$

where $\mathbf{A}$ is the vector potential of light field, $\hat{\mathbf{J}}$ is the current operator, $\mathbf{Q}_n$ is the position vector of site n, and we adopt the atomic units with $c = e = \hbar = 1$. Since the light wavelength is much larger than the system sizes considered in this paper, $\mathbf{A}$ is approximated to be independent of position.

We consider the strong correlation case $U \gg t$ and $U \gg V$ in this paper. For the special case of $t = V = 0$, the energy eigenvalues simply take the values mU, where m is the number of doubly occupied sites, and a huge number of energy eigenstates with different spin configurations are degenerate at each energy level. For finite t and V satisfying the condition $U \gg t$ and $U \gg V$, the degeneracy is lifted and each discrete energy level becomes an energy band. Taking into account the effects of transfer term $\hat{T}$ to the second order in t/U, H_{e} can be approximated to the equation

$$H_{\mathrm{e}} = \sum_{m} H_{\mathrm{eff}}^{(m)}, \tag{8}$$

where $H_{\mathrm{eff}}^{(m)}$ is an effective Hamiltonian for the states in the $(m+1)$th lowest energy band. The effective Hamiltonians are given by[32,33]

$$H_{\mathrm{eff}}^{(m)} = mUP_m + \hat{V}P_m + P_m\hat{T}P_m - U^{-1}P_m\hat{T}P_{m+1}\hat{T}P_m + U^{-1}P_m\hat{T}P_{m-1}\hat{T}P_m, \tag{9}$$

where P_m is the projection operator onto the Hilbert subspace S_m for the states with m doubly occupied sites. The coefficient of the fourth and fifth terms are modified by introducing $\hat{V}$. However, we take into account the terms up to the second order in t/U and V/U, and neglect the V dependence of them. The second term describes the Coulomb interaction between nearest-neighbor sites. The third term describes the transfer of electrons without changing the number of doubly occupied and empty sites, namely, the transfer of electrons at the doubly (singly) occupied sites to the nearest-neighbor singly occupied (empty) sites. Therefore, this term describes the transfer of photogenerated charges. The fourth term describes the AF Heisenberg spin-spin interaction between nearest-neighbor sites with the coupling constant $J = 4t^2/U$ and the virtual three-site transfer. The fifth term is inherent in the photoexcited states, and describes several different transfer processes of an empty and doubly occupied site pair at the nearest neighbor. This effective Hamiltonian is an extension of the well-known t–J Hamiltonian to the multiphoton excited states.

Here and hereafter we use t as the unit of energy, and $1/t$ as the unit of time. Then, there are three energy scales in $H_{\mathrm{eff}}^{(m)}$. The charge transfer term $P_m\hat{T}P_m$ and the nearest-neighbor Coulomb interaction term $\hat{V}P_m$ are $O(1)$ and $O(V)$, respectively, and the other terms are $O(U^{-1})$.

The light absorption spectrum $\alpha(\omega)$ from the ground state $|\psi_0\rangle$ is given by

$$\alpha(\omega) = -\frac{1}{\pi} \mathrm{Im}\left(\langle \psi_0 | \hat{J}^{\dagger} \frac{1}{\omega + E_0 + i\epsilon - H_{\mathrm{eff}}^{(1)}} \hat{J} | \psi_0 \rangle \right), \tag{10}$$

where ω is the angular frequency of the light, E_0 is the energy eigenvalue of the ground state, ϵ is an artificial broadening factor, $\hat{J}$ is the component of $\hat{\mathbf{J}}$ to the light polarization direction. Here we use the fact that $\hat{\mathbf{J}}|\psi_0\rangle \in S_1$, and therefore only the states which belong to the subspace S_1 contribute to $\alpha(\omega)$. The equation (10) is numerically evaluated by the Lanczos method.[34] We need finite ϵ to obtain converged absorption spectrum by the method. We use the smallest value of ϵ where the converged absorption spectra are obtained for all the Coulomb parameters.

We also calculate the free induction decay (FID) intensity after the excitation by an ultrashort laser pulse. It is given by[35]

$$I(\tau) = |\langle \psi_0 | \hat{J} \exp(-iH_{\mathrm{eff}}^{(1)}\tau) \hat{J} | \psi_0 \rangle|^2, \tag{11}$$

where τ is time elapsed after the pulse.

The light absorption spectrum $\alpha(\omega)$ is given by the Fourier transformation of the square root of $I(\tau)$. However, these two physical quantities often provide us with complementary information in the practical numerical calculations. We need to use relatively large ϵ to calculate $\alpha(\omega)$ with using Eq. (10). As a results, we obtain smeared $\alpha(\omega)$ across the frequency range of ϵ, and information about some fine structures is lost. We do not need to assume an artificial broadening or damping factor to calculate $I(\tau)$ with using Eq. (11). Therefore, we can obtain fine structure information which is lost in $\alpha(\omega)$ by analyzing $I(\tau)$.

III. RESULTS AND DISCUSSION

In the following analysis, the half-filled case is considered. In the 2D case, a square lattice with the system size $N=26$ is considered, and the periodic boundary condition is used. In the 1D case, a chain with $N=26$ is considered, and the periodic boundary condition is used. The light field is assumed to be polarized in the direction of a side of the square lattice in the 2D case, and in the direction of chain in the 1D case.

Here we discuss the validity of $H_{\mathrm{eff}}^{(m)}$ as the effective Hamiltonian for the extended Hubbard model. For this purpose, we compare $\alpha(\omega)$ obtained with using the effective Hamiltonian and the original extended Hubbard Hamiltonian in the 2D case with $N=16$. For $U^{-1} \lesssim 0.04$, $H_{\mathrm{eff}}^{(m)}$ well reproduces the results obtained in the extended Hubbard Hamiltonian all through the range $V \lesssim 10$ and $V \lesssim U/4$. Note that the ground state changes from the Mott insulator to the CDW state as V is increased beyond a critical value around $V=U/4$. Around $U^{-1}=0.1$, the difference in $\alpha(\omega)$ becomes prominent. However, qualitatively the same results for $\alpha(\omega)$ are obtained for $V \lesssim U/4$ at $U^{-1}=0.1$. Therefore, we can suppose that $H_{\mathrm{eff}}^{(m)}$ is appropriate as the effective Hamiltonian for the extended Hubbard model in the parameter range $U^{-1} \lesssim 0.1, V \lesssim 10$, and $V \lesssim U/4$. We consider this parameter region in the following.

In the Lanczos method, a few lowest energy eigenstates are obtained by considering the linear combinations of the Krylov sequence of Hamiltonian. By considering the Krylov sequence of $(H_{\mathrm{eff}}^{(1)}-E)^2$ instead of $H_{\mathrm{eff}}^{(1)}$, we obtain a few energy eigenstates of $H_{\mathrm{eff}}^{(1)}$ whose energy eigenvalues are closest to a constant E. To investigate the physical properties of the energy eigenstates which are responsible for the main structures in $\alpha(\omega)$, we numerically calculate some energy eigenstates by the extended Lanczos method, and analyze the charge correlation function $\zeta(r)$ and the spin correlation function $\eta(r)$ defined by the following equations:

$$\zeta(r) = \langle \psi_p | d_n d_m | \psi_p \rangle, \tag{12}$$

$$\eta(r) = \langle \psi_p | \mathbf{S}_n \cdot \mathbf{S}_m | \psi_p \rangle. \tag{13}$$

Here $|\psi_p\rangle$ is an energy eigenstate, $d_n = 1 - \Sigma_\sigma c_{n,\sigma}^\dagger c_{n,\sigma}$ and $\mathbf{S}_n$ are the charge density and spin operators at the nth site, respectively, r is the distance between the sites n and m, and unit of distance is the lattice spacing. Furthermore, we define the following spin correlation function in the 1D case:[36]

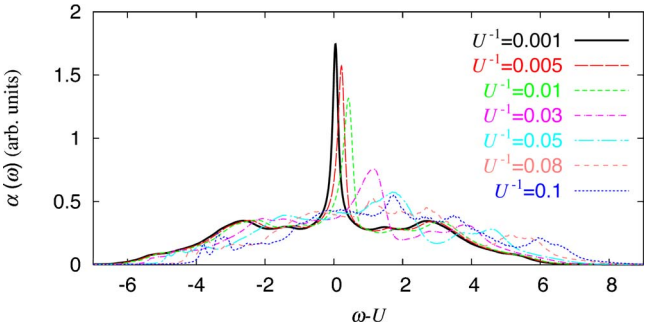

FIG. 1. (Color online) The absorption spectra $\alpha(\omega)$ at $V=0$ for the various values of U^{-1} in the 2D case. The artificial broadening $\epsilon=0.1$ is used.

$$\tilde{\eta}(r) = \langle \psi_p | \sum_{l=0}^{2} \tilde{P}_l \mathbf{S}_0 \cdot \mathbf{S}_{r+l} \tilde{P}_l | \psi_p \rangle. \tag{14}$$

Here $\tilde{P}_l$ is the projection operator onto the subspace where there are l doubly occupied or empty sites between the 0th and $r+l$th sites. If spin-charge separation is complete, $\tilde{\eta}(r)$ is the spin correlation function of the separated spin wave function.

There exist neither empty nor doubly occupied sites in the ground state, and pairs of empty and doubly occupied sites are generated by photoexcitation within the present strong correlation model. It is not appropriate to describe these photogenerated charges by holes and electrons, and they are more properly described by holons and doublons.[2,34] We therefore use the terminology holons and doublons to describe the charges associated with the empty and doubly occupied sites in SCLDES. However, we do not claim by this terminology that complete spin-charge separation holds. Note that there is one pair of a holon and a doublon in the energy eigenstates which contribute to absorption spectrum.

A. Hubbard model

We begin with the case that only the on-site Coulomb interaction is considered ($V=0$) in this section. We show the numerical results for $\alpha(\omega)$ for the various values of U^{-1} in Fig. 1.

We first consider the very strong correlation region $U^{-1} \lesssim 0.01$ in order to focus our attention to the essential properties inherent in the strongly correlated 2D Mott insulators. As seen from Fig. 1, the following features are observed: (i) The absorption spectrum is widely distributed in the range of $-8 \lesssim \omega - U \lesssim 8$. (ii) There are sharp peaks near $\omega - U = 0$, and two broad peaks around $\omega - U = \pm 2.7$. (iii) As U^{-1} is increased, the central peak blueshifts, and the width of the peak increases. (iv) Except for the central peak structure, $\alpha(\omega)$ is nearly independent of U.

In order to clarify the above characteristic features in the absorption spectrum for the 2D Mott insulators, it is instructive to compare Fig. 1 to the results for the transient coherent optical response calculated for the same effective Hamiltonian. In our previous paper,[35] a well-separated two-step relaxation and a quantum beat have been observed in tran-

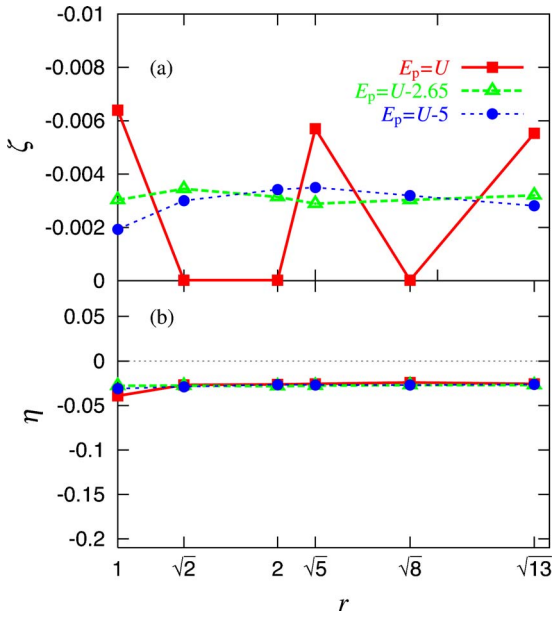

FIG. 2. (Color online) (a) The charge correlation function $\zeta(r)$ and (b) the spin correlation function $\eta(r)$ for $|\psi_p\rangle$ with the energy eigenvalues $E_p-U=0$ (the central peak), -2.65, and -5, at $U^{-1}=0.001$ and $V=0$ in the 2D case.

sient four wave mixing (TFWM) and FID. The slower spin relaxation follows the faster charge relaxation as a result of the coupling between the spin and charge degrees of freedom, and we can clarify the interplay of charge and spin degrees of freedom by analyzing these coherent optical transient phenomena. The charge relaxation time and the period of the quantum beat are nearly independent of U, and they are approximately equal to the inverses of the bandwidth of $\alpha(\omega)$ and the energy difference between the two broad peaks multiplied by 2π, respectively. Therefore, the ultrafast charge relaxation and the quantum beat correspond to the wide bandwidth and the broad peak structure in $\alpha(\omega)$, respectively. The width of the central peak shown in Fig. 1 is very close to the artificial width ϵ for $U^{-1} \lesssim 0.005$. Since we here obtain smeared $\alpha(\omega)$ with using Eq. (10), this result just shows that the width of the peak is less than ϵ. This is consistent with the spin relaxation time in the U^{-1} region. Around $U^{-1}=0.01$, the width of the central peak is estimated to be approximately equal to the inverse of the spin relaxation time multiplied by 2π. Since we can find no other sharp structure in $\alpha(\omega)$, we can conclude that the slower spin relaxation corresponds to the central peak.

To understand these characteristic features, we calculate energy eigenstates which are responsible for these structures. We show the charge and spin correlation functions $\zeta(r)$ and $\eta(r)$ for several energy eigenstates at $U^{-1}=0.001$ in Fig. 2. As seen from this figure, $\zeta(r)$ and $\eta(r)$ are approximately constant irrespective of the energy in the broad absorption band, except for the energy eigenstates which are responsible for the central peak. From the analysis of the TWFM and FID, it has been shown that the spin relaxation is basically exponential, and therefore, the relaxation is interpreted as the irreversible phase relaxation to which almost infinite number of energy eigenstates contribute.[35] Therefore, the central peak arises from the excitation to almost infinite number of energy eigenstates. Actually, we obtain many energy eigenstates in the spectral region of the central peak. The calculated energy eigenstates are classified into two categories. Some have approximately constant $\zeta(r)$ and $\eta(r)$, and the other ones have the characteristic $\zeta(r)$ mentioned bellow. We show $\zeta(r)$ and $\eta(r)$ for the latter case in Fig. 2. As seen from this figure, $\zeta(r)$ is almost zero at the site pairs which belong to the same bipartite sublattice, and $\eta(r)$ is approximately constant.

These results can be understood as follows. For $U^{-1} \lesssim 0.01$, the charge transfer term $P_1\hat{T}P_1$ is dominant in $H_{\text{eff}}^{(1)}$ because only this term is $O(1)$ and the other ones are $O(U^{-1})$. We here consider the eigenstates of $P_1\hat{T}P_1$ because the eigenstates of $H_{\text{eff}}^{(1)}$ are approximated well by them. The term can be rewritten as

$$P_1\hat{T}P_1 = -\sum_d (\tilde{T}_d + \tilde{T}_{-d}), \tag{15}$$

$$\tilde{T}_d = \sum_{n,\sigma} P_1 c^{\dagger}_{n(d),\sigma} c_{n,\sigma} P_1, \tag{16}$$

where $n(\pm d)$ is the nearest-neighbor site of the site n in the directions of $\pm d$, and $d=x,y$. The operator $\tilde{T}_d$ transfers a holon (doublon) at the site n to the site $n(-d)$ $(n(d))$, and simultaneously transfers a spin at the site $n(-d)$ $(n(d))$ to the site n. Therefore, $\tilde{T}_d$ is not a simple charge transfer term, and not only the charge positions but also the background spins are altered by operating $\tilde{T}_d$.

We first consider the eigenstates of $\tilde{T}_d$ in the simple case where there is a single holon or doublon. Since $\tilde{T}_d$ is unitary, the eigenvalue equation can be written as

$$\tilde{T}_d|\Psi(\mathbf{q})\rangle = \exp(iq_d)|\Psi(\mathbf{q})\rangle, \tag{17}$$

where q_d is the component of $\mathbf{q}$ in the direction of d. As seen from Eq. (15), $|\Psi(\mathbf{q})\rangle$ is also an eigenstate of $P_1\hat{T}P_1$ with an eigenvalue

$$E^{(\text{CTT})}(\mathbf{q}) = -2\sum_d \cos q_d. \tag{18}$$

As mentioned before, since only one spin is altered by the transfer, the spin scattering induced by $\tilde{T}_d$ is a higher-order process of $O(1/N)$. As a result, $\mathbf{q}$ can be written as

$$\mathbf{q} = \mathbf{q}_i + \mathbf{\Delta q}_i(s), \tag{19}$$

where $\mathbf{q}_i$ are the discrete momentums which are compatible with the periodic boundary condition. The deviations $\mathbf{\Delta q}_i(s)$ are $O(1/N)$,[37] and depend on the spin structure which is labeled by the index s. Since $\tilde{T}_d$ is lattice translation operator for a holon (doublon) in the $-d$ (d) direction neglecting the spin scattering of the $O(1/N)$ process, $-\mathbf{q}$ $(\mathbf{q})$ can be regarded as the quasimomentum of a holon (doublon). Thus, $\mathbf{q}^{(\text{spin})}=\mathbf{k}+\mathbf{q}$ $(\mathbf{q}^{(\text{spin})}=\mathbf{k}-\mathbf{q})$ can be regarded as the quasimomentum of the spin system, where $\mathbf{k}$ is the total momentum.

From Eq. (17), we can show that a spin and charge configuration $|\phi\rangle$ and $(\Pi_{l=1}^{L}\tilde{T}_{d(l)})|\phi\rangle$ are superposed with the equal weight in $|\Psi(\mathbf{q})\rangle$. Since the AF spin order is destroyed by operating $\Pi_{l=1}^{L}\tilde{T}_{d(l)}$ when L is large enough, $|\Psi(\mathbf{q})\rangle$ do not have the AF spin order.

We next consider the photoexcited states, where there exist a holon and a doublon. Neglecting the collision between the holon and the doublon, which is also the process of $O(1/N)$, the eigenvalues are given by

$$E^{(\mathrm{CTT})}(\mathbf{q}^{(\mathrm{H})},\mathbf{q}^{(\mathrm{D})}) \cong -2\sum_{d}\{\cos q_d^{(\mathrm{H})} + \cos q_d^{(\mathrm{D})}\}, \quad (20)$$

where $-\mathbf{q}^{(\mathrm{H})}$and $\mathbf{q}^{(\mathrm{D})}$ are the quasimomentums of the holon and the doublon, respectively. The bandwidth given by Eq. (20) is 16, and this value is consistent with that of $\alpha(\omega)$ obtained in our numerical calculations. The total momentum $\mathbf{k}$ can be written as

$$\mathbf{k} = -\mathbf{q}^{(\mathrm{H})} + \mathbf{q}^{(\mathrm{D})} + \mathbf{q}^{(\mathrm{spin})}. \quad (21)$$

As shown in Eq. (19), the quasimomentums satisfy $\mathbf{q}^{(\mathrm{H})} = \mathbf{q}_i + O(1/N)$ and $\mathbf{q}^{(\mathrm{D})} = \mathbf{q}_j + O(1/N)$. Therefore, a large number of the energy eigenstates are nearly degenerate to the value $E^{(\mathrm{CTT})}(\mathbf{q}_i,\mathbf{q}_j)$, and the deviations from the value are $O(1/N)$. These nearly degenerate energy eigenstates have nearly the same quasimomentums of a holon and a doublon, but different spin structures. This does not imply the full spin-charge separation. For example, the charge transfer motion destroys the AF spin order, and all the energy eigenstates do not have the order as shown before. Note that the numbers of the nearly degenerate energy eigenstates are huge; they are about the dimension of the Hilbert space divided by N^2 because the charge degrees of freedom are $O(N^2)$.

This picture is consistent with our results that $\zeta(r)$ and $\eta(r)$ are approximately constant except for the energy eigenstates contributing to the central peak. Furthermore, the characteristic charge structure of these energy eigenstates can be explained within the picture, as shown in the following.

We consider the energy eigenstates with $|q_x^{(\mathrm{H})}| = |q_y^{(\mathrm{H})}| = |q_x^{(\mathrm{D})}| = |q_y^{(\mathrm{D})}| \simeq \pi/2$, where $E^{(\mathrm{CTT})}(\mathbf{q}^{(\mathrm{H})},\mathbf{q}^{(\mathrm{D})}) \cong 0$. In this case, we can construct the energy eigenstates where a holon (doublon) exist only on one bipartite lattice by considering the linear combinations of degenerate ones. Then, the condition that a holon and a doublon cannot occupy the same site simultaneously plays an important role. Because of the rule, if a holon is in one bipartite sublattice, then a doublon must be in the other bipartite sublattice in this case. As a result, $\zeta(r)$ vanishes at the site pairs which belong to the same bipartite sublattice for the states given by the linear combination of the states with $|q_x^{(\mathrm{H})}| = |q_y^{(\mathrm{H})}| = |q_x^{(\mathrm{D})}| = |q_y^{(\mathrm{D})}| \simeq \pi/2$. This agrees well with the characteristic $\zeta(r)$ observed in the energy eigenstates contributing to the central peak.

We also numerically calculate the transition moments from the ground state to various energy eigenstates. We find that the transition moments for the energy eigenstates given by the linear combination of the states with $|q_x^{(\mathrm{H})}| = |q_y^{(\mathrm{H})}| = |q_x^{(\mathrm{D})}| = |q_y^{(\mathrm{D})}| \simeq \pi/2$ are, in general, much larger than those for the other energy eigenstates, and therefore the sharp peak arises partly from the large transition moments for these states. The large transition moments can be attributed to the characteristic charge structure of these states as shown below. As seen from Eqs. (6) and (7), $H_{e\text{-}p}$ transfers an antiparallel spin pair at the nearest-neighbor sites to a pair of empty and doubly occupied sites. Therefore, the transition moment between the ground state and an energy eigenstate is expected to be large in the following two cases: (i) the spin structure of the state is close to that of the ground state, and (ii) $\zeta(1)$ for the state, which shows the probability that a holon and a doublon are located at the nearest-neighbor sites, is large. Because of the characteristic charge structure, $\zeta(1)$ for these states are much larger than those for the other energy eigenstates.

Furthermore, the density of states at $\omega = U$ diverges as N tends to ∞ when the terms of $O(1/N)$ are neglected. The central peak arise also partly from the divergence. This divergence can be understood as follows. Only the energy eigenstates with the total momentum $\boldsymbol{k}=0$ can be photoexcited because the ground state has zero momentum. Then, $\mathbf{q}^{(\mathrm{H})} = \mathbf{q}^{(\mathrm{D})} + \mathbf{q}^{(\mathrm{spin})}$ holds. When $|q_x^{(\mathrm{spin})}| = |q_y^{(\mathrm{spin})}| = \pi$, $E^{(\mathrm{CTT})}(\mathbf{q}^{(\mathrm{H})},\mathbf{q}^{(\mathrm{D})}) = 0$ holds irrespective of $\mathbf{q}^{(\mathrm{H})}$ and $\mathbf{q}^{(\mathrm{D})}$. Moreover, there are also two shoulders in the density of states around the energies of the two broad peaks, and the broad peaks arise from this structure.

The quasidegeneracy of the energy eigenstates with nearly the same quasimomentums is lifted by the spin-spin interaction, and the difference in the energy among them is proportional to spin-spin interaction constant $J = 4U^{-1}$. As a result, the width of the central peak is approximately proportional to U^{-1} except for the case where U^{-1} is extremely small. This agrees with the dependence of the spin relaxation time on U^{-1} obtained in TFWM and FID.

Next we consider the region $U^{-1} \gtrsim 0.02$, in which the characteristic $\alpha(\omega)$ in the extremely strong correlation region is not clearly seen. The central peak is broadened and becomes unclear as U^{-1} is increased, and the U^{-1} dependence becomes prominent besides the central peak structure. We also calculate $\zeta(r)$ and $\eta(r)$ for various energy eigenstates. We show $\zeta(r)$ and $\eta(r)$ for $|\psi_p\rangle$ where E_p are equal to the energies of the two small peaks in the low energy region at $U^{-1} = 0.1$ in Fig. 3. As in the case of $U^{-1} \lesssim 0.01$, $\zeta(r)$ for all the calculated eigenstates are approximately constant. However, $\eta(r)$ are different from those in the case of $U^{-1} \lesssim 0.01$. Some energy eigenstates have AF spin order in the low energy region as seen from Fig. 3, and the energy region increases as U^{-1} is increased. Except for these lower energy eigenstates, $\eta(r)$ are approximately constant, and therefore the energy eigenstates do not have the AF spin order. The energy eigenstates contributing to the broad central peak do not have the charge structure inherent in the sharp central peak for $U^{-1} \lesssim 0.01$. As a result, the transition moments for these states are comparable to those for the other energy eigenstates.

As mentioned before, the charge transfer term is dominant for $U^{-1} \lesssim 0.01$. However, these results show that the effect of the spin-spin interaction on the energy eigenstates becomes prominent for $U^{-1} \gtrsim 0.02$. Some energy eigenstates in the lower energy region have the AF spin order to gain the spin-

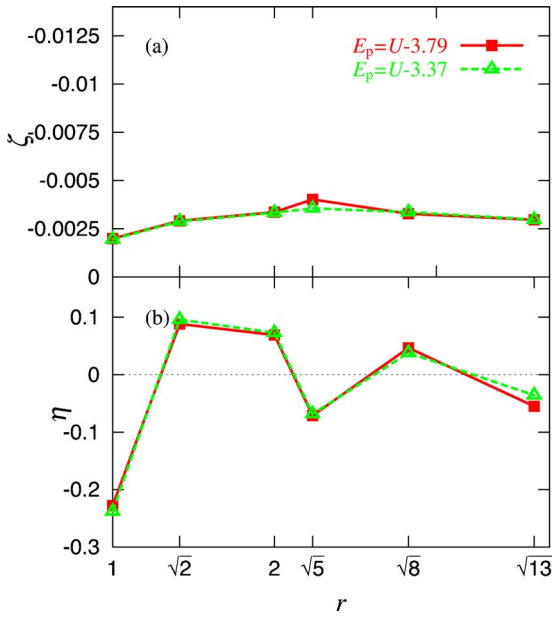

FIG. 3. (Color online) (a) The charge correlation function $\zeta(r)$ and (b) the spin correlation function $\eta(r)$ for $|\psi_p\rangle$ where the energy eigenvalues E_p are equal to the energies of the two small peaks in the low energy region ($E_p-U=-3.79$ and -3.37) at $V=0$ and $U^{-1}=0.1$ in the 2D case.

spin interaction energy, and the quasidegeneracy inherent in the very strong correlation region is destroyed. Furthermore, the prominent dependence of $\alpha(\omega)$ on U^{-1} for $U^{-1}\gtrsim 0.02$ can be attributed to this.

We calculate $\alpha(\omega)$ also in the 1D system with the same system size. The dependence of $\alpha(\omega)$ on U^{-1} is very weak in the strong correlation region $U^{-1}\leqslant 0.1$, and the results at $U^{-1}=0.01$ are shown in Fig. 4. There are 12 main peaks. These main peaks are Lorentzian and the widths of the peaks are equal to ϵ used in Eq. (10). Furthermore, we calculate the energy eigenstates at the peak energies of the main peaks, and find that the magnitude of transition moment for each energy eigenstate is the same as that of the total transition moment of the corresponding peak. Therefore, each main peak is due to the excitation to a single energy eigenstate. The discrete absorption spectrum is a result of a finite size effect. Note, however, that the dimension of $H^{(1)}_{\rm eff}$ is the order of 10^7 both in the 2D and 1D cases, and therefore continuous

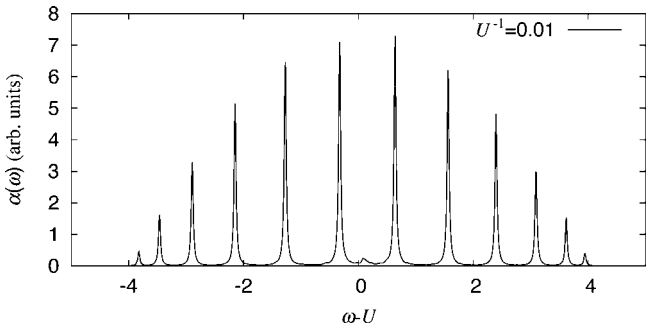

FIG. 4. The absorption spectrum $\alpha(\omega)$ at $V=0$ and $U^{-1}=0.01$ in the 1D case. The artificial broadening $\epsilon=0.02$ is used.

absorption spectra are obtained in the 2D case even when the same value of ϵ is used. Therefore, the discreteness in $\alpha(\omega)$ observed in the cluster calculations should be regarded as a characteristic of the 1D system.

The spin correlation functions $\tilde{\eta}(r)$ for these 12 energy eigenstates are similar to that of the AF ground state. Furthermore, $\tilde{\eta}(r)$ for these energy eigenstates are almost identical, although $\zeta(r)$ are so different. This shows that the spin and charge structures are not correlated and spin-charge separation holds almost rigorously in these energy eigenstates. This further shows that only the energy eigenstates with a specific spin wave function can be photoexcited. Therefore, only a quite small portion of the energy eigenstates dominates the transition moment from the ground state. This is the cause of the discrete absorption spectrum. As a result of the spin-charge separation in the 1D case, $\alpha(\omega)$ are so different between the 1D and 2D cases. It should be noted that the optical absorption spectrum sensitively reflects the difference in the spin-charge interplay between the 1D and 2D cases.

We here mention how the difference in the optical absorption spectrum between the 1D and 2D cases, appears in the dynamics of the state excited by laser pulse. Just after the pulse excitation, a holon and a doublon are generated at the nearest neighbor sites as seen from Eqs. (6) and (7), and the AF spin configuration is destroyed only locally at these sites. Therefore, the system has the AF order just after the pulse excitation. This, however, does not contradict to the fact that the energy eigenstates do not have the AF spin order in the 2D case as shown below. In the 2D case, the energy eigenstates with nearly the same quasimomenta of a holon and a doublon, but with different spin structures, are nearly degenerate in energy, and the difference in the energy eigenvalues among them is $O(1/N)$, as shown before. All the spin configurations for the one-photon excited states with a holon and a doublon, are included in Hilbert space spanned by these nearly degenerate energy eigenstates, and therefore the AF spin state is obtained by a linear combination of these nearly degenerate energy eigenstates. In the pulse excitation process, many energy eigenstates are coherently excited, and the excited state has the AF spin order just after the excitation, even when the ground state is resonantly excited to the energy eigenstates in very small energy range. However, since almost infinite number of the energy eigenstates with different spin structures are photoexcited, relaxation occurs, and the AF spin order becomes weaker as time goes on. In contrast to this, in the 1D case, only the discrete energy eigenstates with the same spin structure are photoexcited due to the spin-charge separation. As a result, $\tilde{\eta}(r)$, and therefore the magnitude of the AF spin order is almost constant in time. In this way, the essential difference in the absorption spectrum between the 1D and 2D cases, is closely related to the difference in the relaxation process. We confirm these results by numerical calculation, and the result in the case of the short laser pulse is discussed in detail in our previous paper.[38]

B. Charge binding effect

We consider the effect of the Coulomb interaction between the nearest-neighbor sites on the photoexcited states in this section.

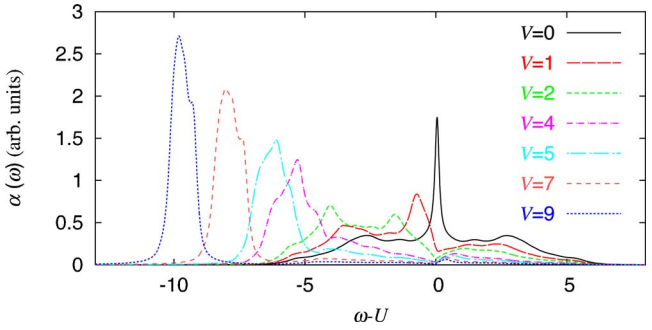

FIG. 5. (Color online) The absorption spectra $\alpha(\omega)$ at $U^{-1}=0.001$ for the various values of V in the 2D case. The artificial broadening $\epsilon=0.1$ is used.

We first show the results at $U^{-1}=0.001$ in order to focus our attention to the essential feature inherent in the very strong correlation region. We show the dependence of $\alpha(\omega)$ on V at $U^{-1}=0.001$ in Fig. 5. As V is increased, the central peak becomes broad and redshifts as seen in the figure. At the same time, the lower broad peak grows rapidly with increasing V, and becomes dominant for $V \gtrsim 4$. This peak arises from the binding effect of a holon and a doublon, and its characteristics are different from the central peak as will be described later. Two peaks are comparable at $V \approx 2$, and the spectral shape is qualitatively different in the regions $V \lesssim 2$ and $V \gtrsim 2$.

We also show the dependence of the FID intensity $I(\tau)$ on V at $U^{-1}=0.001$ in Fig. 6. As shown previously, the physical origins of the characteristics of $I(\tau)$ at $V=0$ are as follows. The rapid decrease for $\tau \lesssim 1$, oscillation for $1 \lesssim \tau \lesssim 5$, and the exponential decrease for $\tau \gtrsim 5$ are the manifestation of the charge relaxation, the quantum beat, and the spin relaxation, respectively. For $V \lesssim 2$, the characteristic two-step relaxation is preserved. The spin relaxation becomes faster as V is increased, and this corresponds to the broadening of the central peak in $\alpha(\omega)$. For $V \gtrsim 4$, the two-step relaxation is not seen. This is because the new peak becomes dominant and the characteristic absorption spectrum at $V=0$ is destroyed by the Coulomb interaction between the nearest-neighbor sites. The decay of $I(\tau)$ becomes slower as V is increased beyond about 2. This corresponds to the change in $\alpha(\omega)$ that the

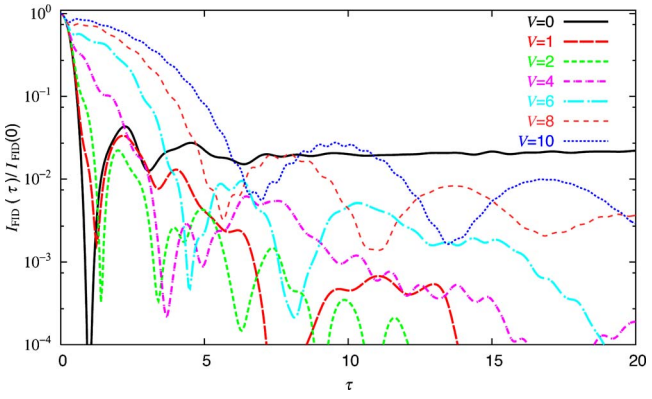

FIG. 6. (Color online) The FID signal $I(\tau)$ at $U^{-1}=0.001$ for the various values of V in the 2D case.

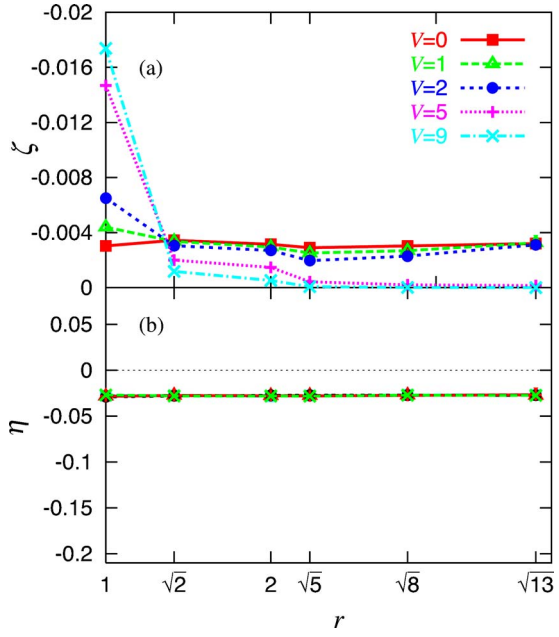

FIG. 7. (Color online) (a) The charge correlation function $\zeta(r)$ and (b) the spin correlation function $\eta(r)$ for $|\psi_p\rangle$ where the energy eigenvalues E_p are equal to the energies of the lower broad peak for $V \leqslant 2$ and the dominant peak for $V \geqslant 4$, at $U^{-1}=0.001$ in the 2D case. The energy eigenvalues $E_p-U=-2.65$, -3.51, -4.03, -6.09, and -9.81 at $V=0$, 1, 2, 5, and 9, respectively.

dominant peak becomes sharper with increasing V. However, even when the V is increased up to 10, $I(\tau)/I(0)$ becomes less than 0.01 for $\tau \gtrsim 10$ as seen from Fig. 6. This shows that a large number of energy eigenstates contribute to the peak. We actually obtained many energy eigenstates in the spectral region of the peak. The transition moments from the ground state to these states are less than 0.1% of the total transition moment of the dominant peak, for example, at $V=8$ and $U^{-1}=0.001$. This small value is consistent with this observation. We observe oscillation in $I(\tau)$ in the large V region. From Fig. 5, we can see that the dominant peak in the large V region consists of several peaks overlapping each other. Since the energy difference between the peak and the largest shoulder is approximately the same as the frequency of the oscillation, the oscillation originates from the multipeak structure.

To understand these characteristic features, we also calculate energy eigenstates at various energies in the band. We first consider the energy eigenstates which contribute to the central peak. The characteristic charge structure of these energy eigenstates observed at $V=0$, disappears when V is increased up to 1.

Next, we consider the energy eigenstates which contribute to the dominant peak for $V \gtrsim 4$, and the lower broad peak for $V \lesssim 2$, which continuously changes to the dominant peak. In Fig. 7, we show $\zeta(r)$ and $\eta(r)$ for the energy eigenstates at the absorption peak for various values of V. As seen from Fig. 7, the magnitude of $\zeta(1)$ increases with increasing V, and $\zeta(r)$ becomes a decreasing function for $V \gtrsim 2$. For $V \gtrsim 5$, $\zeta(r)$ almost vanishes in the long range part $r \geqslant \sqrt{8}$, showing that the photogenerated charges are bound. As seen

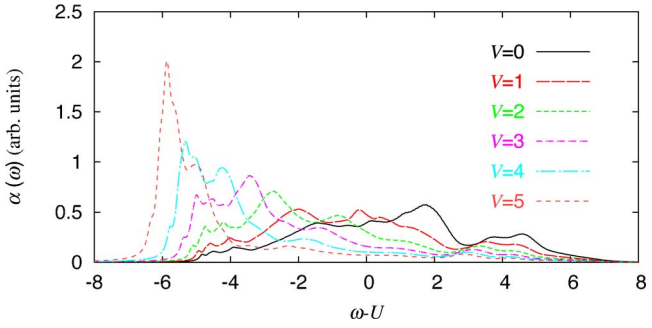

FIG. 8. (Color online) The absorption spectra $\alpha(\omega)$ at $U^{-1}=0.05$ for the various values of V in the 2D case. The artificial broadening $\epsilon=0.1$ is used.

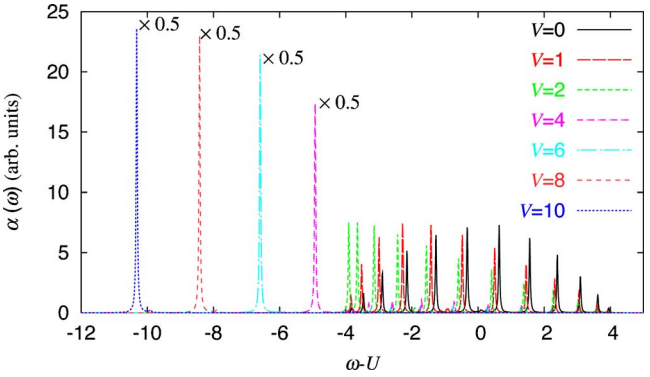

FIG. 9. (Color online) The absorption spectra $\alpha(\omega)$ at $U^{-1}=0.01$ for the various values of V in the 1D case. The artificial broadening $\epsilon=0.02$ is used.

from Fig. 7, $\eta(r)$ are approximately constant, and the correlation between spin and charge structures is very weak.

We calculated the energy eigenstates not only at the peak but also at the shoulders of the dominant peak. We obtain many energy eigenstates which are nearly degenerate to the energy of each fine structure. The charge correlation functions $\zeta(r)$ for these nearly degenerate states are almost identical, and $\eta(r)$ for them are approximately constant, and the deviation of $\eta(r)$ between these states is much larger than that of $\zeta(r)$. Therefore, we can conclude that the energy eigenvalues are mainly determined by the charge structure, and large numbers of the energy eigenstates with nearly the same charge but different spin structure are nearly degenerate in energy also in the large V region. Moreover, the calculated energy eigenstates contributing to all the structures in the dominant peak, have monotonously decreasing $\zeta(r)$. This shows that all these energy eigenstates have the charge structure of the lowest bound state with zero node.

Consequently, there are bound states of a holon and a doublon when V is large enough, and the dominant peak in the large V region is due to the excitation to these charge bound states, similar to the case of excitons. However, many energy eigenstates contribute to the dominant peak in this case, and this is in contrast to the case of excitons where only a few exciton states dominate the optical transition moments. We should therefore pay attention to the fact that the holon-doublon bound states in the 2D Mott insulators are coupled with the large number of spin degrees of freedom, and is significantly different from the exciton state in conventional band insulators.

We next consider how the dependence of $\alpha(\omega)$ on V changes for larger values of U^{-1}. We show $\alpha(\omega)$ for several values of V at $U^{-1}=0.05$ in Fig. 8. As V is increased, the lower (higher) side of the broad band increases (decreases) for $V\lesssim 2$. There are two small peaks in $\alpha(\omega)$ at $\omega-U=-4.5$ and -3.9 when $V=0$. These two peaks drastically grow as V is increased, and become dominant around $V=4$. This is different from the case of $U^{-1}=0.001$ where the lower broad peak changes to the dominant peak. With further increase of V, the dominant peaks become sharper and redshift.

We obtain energy eigenstates in the energy region of the dominant peaks for $V\gtrsim 4$, and the peaks which continuously grow to the dominant peaks for $V\lesssim 2$. From the same discussion as the case of $U^{-1}=0.001$, we can show that the dominant peak for $V\gtrsim 4$ is due to the excitation to many charge bound states. However, the deviations in $\zeta(r)$ among the energy eigenstates contributing to the dominant peaks are much larger at $U^{-1}=0.05$ than at $U^{-1}=0.001$. This shows that the charge structures for these states are strongly affected by their spin structures, in contrast to the case of $U^{-1}=0.001$. As for the spin structure, the energy eigenstates responsible for the peaks have AF spin order regardless of the values of V.

The width of the dominant peak in the large V region is smaller at $U^{-1}=0.05$ than at $U^{-1}=0.001$, and the largest transition moments for the energy eigenstates responsible for the dominant peak at $U^{-1}=0.05$ is about 40 times larger than that at $U^{-1}=0.001$ for the same value of V. This shows that the transition moments concentrate on much fewer energy eigenstates at $U^{-1}=0.05$ than at $U^{-1}=0.001$.

For $U^{-1}\gtrsim 0.02$, the dominant peak in the large V region becomes sharper and the number of the energy eigenstates responsible for these peaks decreases, as U^{-1} is increased. The strong U^{-1} dependence of this number can be attributed to the fact that some energy eigenstates have the AF spin order in the U^{-1} region. As mentioned before, the transition moment between the ground state and an energy eigenstate increases as the spin structure of the state is closer to the ground state. Therefore, the states with the strong AF spin order have much larger transition moments from the AF ground state than the other states where the AF order is destroyed.

For $U^{-1}\gtrsim 0.06$, the ground state is the CDW state in the region $V\gtrsim 4$, where the dominant peak due to the holon-doublon bound state is expected. As a result, the characteristic absorption spectrum in the large V region cannot be observed in this U^{-1} region.

On the other hand, $\alpha(\omega)$ is nearly independent of U^{-1} for $U^{-1}\lesssim 0.01$ also in the large V region. This is because the charge transfer and the nearest-neighbor interaction terms in Eq. (9) are dominant in the small U^{-1} and large V region, and both the terms are independent of U^{-1}.

We also calculate the dependence of $\alpha(\omega)$ on V in the 1D case. Since the dependence of $\alpha(\omega)$ on U^{-1} is very weak also for finite V in the strong correlation region $U^{-1}\leqslant 0.1$, only the results at $U^{-1}=0.01$ are shown in Fig. 9. The absorption spectrum is discrete all through the V region considered in

this paper as seen from this figure. From the numerical calculations, we can show that these isolated peaks are due to the excitation to a single energy eigenstate also when V is finite. We calculate $\zeta(r)$ and $\tilde{\eta}(r)$ for the eigenstates responsible for the absorption peaks. We confirm the previous results that a bound state of a holon and a doublon exist for $V \geqslant 2$, and the state dominates the transition moment from the ground state.[10–18] Furthermore, we obtain the following results specific to 1D Mott insulators. The charge correlation functions $\zeta(r)$ are so different between these energy eigenstates, and $\zeta(r)$ significantly changes with V in the low energy part. However, $\tilde{\eta}(r)$ are almost identical between these energy eigenstates, and $\tilde{\eta}(r)$ are nearly independent of V except when a holon and a doublon are bound. The magnitudes of the AF spin order of the energy eigenstate with a bound holon-doublon pair are slightly smaller than those of the other ones. This weak correlation between spin and charge structures occurs because the indirect AF spin-spin interaction between the spin pair across the photogenerated charges is strongly suppressed when a holon and a doublon are strongly bound.[39] Therefore, the correlation can be regarded as a kind of finite size effect, and spin-charge separation almost rigorously holds all through the V region considered in this paper. As a result, a single states dominates the transition moment when V is large enough just like the case of exciton in the 1D band insulators.[40] However, it should be noted that the bound state in 1D Mott insulators consists of spinless charges, a holon and a doublon, which are separated from the spin degrees of freedom (spin-charge separation).

IV. CONCLUSION

In conclusion, the following results are obtained in the 2D case when $V=0$. For $U^{-1} \lesssim 0.01$, the charge transfer term is dominant, and the energy eigenvalues are nearly determined by the quasimomenta of a holon and a doublon. A large number of energy eigenstates which have nearly the same quasimomenta but different spin structures are nearly degenerate in energy. The energy eigenstates do not have AF spin order because the order is destroyed by the charge transfer in the optically excited states. As a result, the following features are observed in $\alpha(\omega)$: the bandwidth is as wide as about 16, and there is a central peak near $\omega=U$. The energy eigenstates responsible for the central peak, have the charge structure where a holon exists in one bipartite sublattice and a doublon exists in the other bipartite sublattice, which results in large transition moments from the ground state for these states. For $U^{-1} \gtrsim 0.02$, the quasidegeneracy is destroyed, and some low energy eigenstates have the AF spin order. This energy region increases with increasing U^{-1}. As a result, the central peak becomes unclear as U^{-1} is increased. As for the effect of the nearest-neighbor Coulomb interaction term, the following results are obtained. Irrespective of the value of U^{-1}, the energy eigenstates where a holon-doublon pair is bound exists, and a dominant peak due to the excitation to these charge bound states, appears in absorption spectrum for $V \gtrsim 4$, unless the transition to the CDW state occurs. In contrast to the case of the conventional excitons, a large number of energy eigenstates have the significant contribution to the dominant peak for $U^{-1} \lesssim 0.01$. These states have nearly the same charge structure but different spin structures, and the large number of states comes from the spin degrees of freedom. These states do not have the AF spin order. As U^{-1} is increased, some of these states begin to have the AF spin order, and optical transition moments concentrate to these states. Even when U^{-1} is increased up to 0.05, many energy eigenstates still have the significant contribution to the dominant peak. This is in contrast to the conventional exciton, and the difference originates from the coupling to the spin degrees of freedom of the whole system. This is also in contrast to the charge bound states in the 1D case, where a single energy eigenstate dominates the optical transition moment as a result of the spin-charge separation. The difference between the 1D and 2D Mott insulators originates from the difference between them in the coupling between spin and charge degrees of freedom.

ACKNOWLEDGMENT

This research was supported by the Japan Society for the Promotion of Science, Grant-in-Aid for Scientific Research Contract No. (C) 15540312.

[1] N. F. Mott, *Metal-Insulator Transitions*, 2nd ed. (Taylor and Francis, London, 1990).

[2] M. Imada, A. Fujimori, and Y. Tokura, Rev. Mod. Phys. **70**, 1039 (1998), and references therein.

[3] See, for example, H. Haug and S. W. Koch, *Quantum Theory of the Optical and Electronic Properties of Semiconductors* (World Scientific, Singapore, 1990).

[4] R. Neudert, M. Knupfer, M. S. Golden, J. Fink, W. Stephan, K. Penc, N. Motoyama, H. Eisaki, and S. Uchida, Phys. Rev. Lett. **81**, 657 (1998).

[5] R. Neudert, S.-L. Drechsler, J. Málek, H. Rosner, M. Kielwein, Z. Hu, M. Knupfer, M. S. Golden, J. Fink, N. Nücker, M. Merz, S. Schuppler, N. Motoyama, H. Eisaki, S. Uchida, M. Domke, and G. Kaindl, Phys. Rev. B **62**, 10752 (2000).

[6] M. Ono, K. Miura, A. Maeda, H. Matsuzaki, H. Kishida, Y. Taguchi, Y. Tokura, M. Yamashita, and H. Okamoto, Phys. Rev. B **70**, 085101 (1981).

[7] S. Mazumdar and Z. G. Soos, Phys. Rev. B **23**, 2810 (1981).

[8] R. M. Fye, M. J. Martins, D. J. Scalapino, J. Wagner, and W. Hanke, Phys. Rev. B **44**, 6909 (1991).

[9] D. Guo, S. Mazumdar, S. N. Dixit, F. Kajzar, F. Jarka, Y. Kawabe, and N. Peyghambarian, Phys. Rev. B **48**, 1433 (1993).

[10] F. B. Gallagher and S. Mazumdar, Phys. Rev. B **56**, 15025 (1997).

[11] F. Gebhard, K. Bott, M. Scheidler, P. Thomas, and S. W. Koch, Philos. Mag. B **75**, 13 (1997).

[12] F. Gebhard, K. Bott, M. Scheidler, P. Thomas, and S. W. Koch, Philos. Mag. B **75**, 47 (1997).
[13] Y. Mizuno, K. Tsutsui, T. Tohyama, and S. Maekawa, Phys. Rev. B **62**, R4769 (2000).
[14] E. Jeckelmann, F. Gebhard, and F. H. L. Essler, Phys. Rev. Lett. **85**, 3910 (2000).
[15] N. Tomita and K. Nasu, Phys. Rev. B **63**, 085107 (2001).
[16] F. H. L. Essler, F. Gebhard, and E. Jeckelmann, Phys. Rev. B **64**, 125119 (2001).
[17] E. Jeckelmann, Phys. Rev. B **67**, 075106 (2003).
[18] H. Matsueda, T. Tohyama, and S. Maekawa, Phys. Rev. B **70**, 033102 (2004).
[19] W. Stephan and K. Penc, Phys. Rev. B **54**, R17269 (1996).
[20] Z. Shuai, S. K. Pati, W. P. Su, J. L. Brédas, and S. Ramasesha, Phys. Rev. B **55**, 15368 (1997).
[21] Z. Shuai, J. L. Brédas, S. K. Pati, and S. Ramasesha, Phys. Rev. B **58**, 15329 (1998).
[22] S. S. Kancharla and C. J. Bolech, Phys. Rev. B **64**, 085119 (2001).
[23] W. Barford, Phys. Rev. B **65**, 205118 (2002).
[24] W. Stephan and P. Horsch, Phys. Rev. B **42**, 8736 (1990).
[25] D. Poilblanc, Phys. Rev. B **44**, 9562 (1991).
[26] E. Dagotto, A. Moreo, F. Ortolani, D. Poilblanc, and J. Riera, Phys. Rev. B **45**, 10741 (1992).
[27] H. Eskes, A. M. Oles, M. B. J. Meinders, and W. Stephan, Phys. Rev. B **50**, 17980 (1994).
[28] J. A. Riera and E. Dagotto, Phys. Rev. B **50**, 452 (1994).
[29] R. Eder, P. Wróbel, and Y. Ohta, Phys. Rev. B **54**, R11034 (1996).
[30] H. Nakano and M. Imada, J. Phys. Soc. Jpn. **68**, 1458 (1998).
[31] T. Tohyama, Y. Inoue, K. Tsutsui, and S. Maekawa, Phys. Rev. B **72**, 045113 (2005).
[32] A. Takahashi, H. Gomi, and M. Aihara, J. Lumin. **94-95**, 499 (2001).
[33] A. Takahashi, S. Yoshikawa, and M. Aihara, Phys. Rev. B **65**, 085103 (2002).
[34] E. Dagotto, Rev. Mod. Phys. **66**, 763 (1994).
[35] A. Takahashi, H. Gomi, and M. Aihara, Phys. Rev. B **69**, 075116 (2004).
[36] M. Ogata and H. Shiba, Phys. Rev. B **41**, 2326 (1990).
[37] K. Kusakabe and H. Aoki, Phys. Rev. B **50**, 12991 (1994).
[38] A. Takahashi, H. Gomi, and M. Aihara, Phys. Rev. Lett. **89**, 206402 (2002).
[39] Hiroki Gomi, Akira Takahashi, Toshihiro Ueda, Hisashi Itoh, and Masaki Aihara, Phys. Rev. B **71**, 045129 (2005).
[40] S. Abe, J. Phys. Soc. Jpn. **58**, 62 (1989).